The Product of the *het-C* Heterokaryon Incompatibility Gene of *Neurospora crassa* Has Characteristics of a Glycine-Rich Cell Wall Protein

Sven J. Saupe, Gretchen A. Kuldau,[1] Myron L. Smith[2] and N. Louise Glass

Botany Department and Biotechnology Laboratory, University of British Columbia, Vancouver, British Columbia, V6T 1W5, Canada

Manuscript received February 15, 1996
Accepted for publication April 22, 1996

ABSTRACT

Filamentous fungi are capable of hyphal fusion, but heterokaryon formation between different isolates is controlled by specific loci termed *het* loci. Heterokaryotic cells formed between strains of different *het* genotype are rapidly destroyed or strongly inhibited in their growth. In *Neurospora crassa*, at least 11 loci, including the mating type locus, affect the capacity to form a heterokaryon between different isolates. In this report, we describe the molecular characterization of the vegetative incompatibility locus, *het-C*. The *het-C*^{OR} allele was cloned by genetically identifying the *het-C* locus in a chromosome walk, and the activity of clones containing the *het-C*^{OR} allele was tested in a functional transformation assay. The *het-C*^{OR} allele encodes a 966-amino acid polypeptide with a putative signal peptide, a coiled-coil motif and a C-terminal glycine-rich domain, similar to glycine-rich domains detected in various extracellular and structural cell envelope proteins. Both the coiled-coil and one-third of the glycine-rich carboxyl terminal domains were required for full *het-C*^{OR} activity. Mutants of *het-C*^{OR} were obtained by repeat-induced point mutation (RIP); these mutants were indistinguishable from wild type during vegetative growth and sexual reproduction but displayed dual compatibility with both of two mutually incompatible *het-C*^{OR} and *het-c*^{PA} strains.

THE ability to distinguish self *vs.* nonself is an attribute of numerous living organisms and is critical in the development and maintenance of multicellular forms. In filamentous fungi, the ability to distinguish self and nonself is essential because of their capacity to undergo hyphal fusion, either within an individual colony or between hypha of different individuals. To maintain individual identity, filamentous fungi possess systems that restrict heterokaryon formation between genetically dissimilar individuals. Heterokaryon compatibility is controlled by specific loci termed *het* (for heterokaryon incompatibility) or *vic* (vegetative incompatibility) loci (for recent reviews see GLASS and KULDAU 1992; LESLIE 1993; BEGUERET *et al.* 1995).

Two strains that contain alternate alleles at a *het* locus can undergo hyphal fusion, but the heterokaryotic cells are rapidly destroyed by a lytic process or are inhibited in their growth (GARNJOBST and WILSON 1956; MYLYK 1975). A given fungal species generally has numerous *het* loci and a genetic difference between individuals at any one of these loci is sufficient to trigger incompatibility and result in a failure to establish a productive heterokaryon. As a consequence, heterokaryon formation between different natural isolates of a given species is unlikely (MYLYK 1976).

Corresponding author: N. Louise Glass, University of British Columbia, Biotechnology Laboratory, Room 237 Wesbrook Bldg., 6174 University Blvd., Vancouver, B.C. V6T 1Z3, Canada.
E-mail: glass@unixg.ubc.ca

[1] *Present address:* Department of Plant Pathology, University of Kentucky, Lexington, KY 40346-0091.

[2] *Present address:* Department of Biology, Carleton University, Ottawa, ON K1S 5B6, Canada.

Genetic determinants that limit heterokaryon formation have been well studied in *Neurospora crassa* (MYLYK 1975; PERKINS 1975); at least 11 loci, including the mating-type locus, regulate the capacity to form productive heterokaryons between different isolates (PERKINS 1988). The mating-type locus differs from other *het* loci in *N. crassa* in that it also regulates entry into sexual reproduction (BEADLE and COONRADT 1944; SANSOME 1946).

In this study, we show the cloning of the heterokaryon incompatibility locus *het-C* from *N. crassa* and describe the functional characterization of the *het-C*^{OR} allele. This is the first report of the isolation of a *N. crassa* gene exclusively involved in vegetative incompatibility. The *het-C* locus was originally identified in forced heterokaryons (GARNJOBST 1953) and then further characterized by using translocation strains generating duplications of the *het-C* locus (PERKINS 1975). Incompatible heterokaryons or partial diploids heterozygous for *het-C* display a slow-growing, curly, flat, aconidiating morphology (Figure 1). The *het-C* incompatible phenotype is less severe than for other *het* gene interactions in which the incompatible heterokaryons (or partial diploids) can be completely inhibited in their growth (MYLYK 1975).

The *het-C*^{OR} allele was cloned by genetically identifying the *het-C* locus in a chromosome walk. The activity of clones containing the *het-C*^{OR} allele was tested in a functional transformation assay by creating synthetic partial diploids for *het-C*. Mutants of *het-C*^{OR} were obtained by repeat-induced point mutation (RIP) (SELKER 1990). Structural and functional analyses of the *het-C*^{OR}

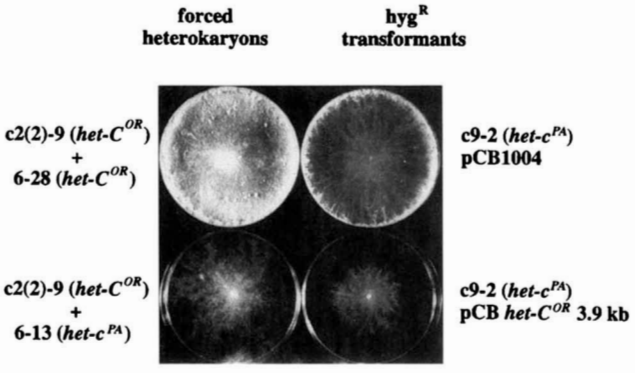

FIGURE 1.—Growth characteristics of a *het-c^{PA}* transformant carrying the *het-C^{OR}* construct as compared to a vector control and compatible and incompatible *het-C* heterokaryons. The figure compares the phenotype of a compatible *het-C* heterokaryon (top left), an incompatible *het-C* heterokaryon (bottom left), a C9–2 (*het-c^{PA}*) transformant containing the pCB1004 vector (top right), and a transformant containing the pCB1004 vector with the 3.9-kb *PstI-SacI het-C^{OR}* fragment (bottom right). All are shown after 3 days incubation at 30° on solid Vogel's medium (transformation plates contain 250 units/ml of hygromycin). The designation of the strains composing the heterokaryons is given.

allele and the phenotype of the RIP mutants has allowed the development of a testable hypothesis concerning interaction of *het-C* gene products and the molecular basis of self/nonself recognition.

MATERIALS AND METHODS

Strains, media and culture methods: A list of the *N. crassa* strains used in this study is given in Table 1, together with their origin and relevant genotypes. The two incompatible alleles of the *het-C* locus are historically designated *het-C* and *het-c* (GARNJOBST 1953). Herein, the two incompatible alleles are designated by superscript *het-C^{OR}* (Oak Ridge) and *het-c^{PA}* (Panama) to refer to the strain of origin.

Vogel's (VOGEL 1964) and Westergaard's (WESTERGAARD and MITCHELL 1947) synthetic media were used for vegetative cultures and crosses, respectively. Heterokaryon compatibility tests were performed by spotting conidial suspensions of auxotrophic strains with complementary requirements on Vogel's minimal agar medium. Strains forming vigorous conidiating cultures after 3 days at 30° were considered compatible. Growth rates were measured by linear growth in race tubes as described (DAVIS and DE SERRES 1970).

Nucleic acid isolation and hybridization: Genomic *N. crassa* DNA was isolated as described in OAKLEY *et al.* (1987). RNA was extracted according to LOGEMANN *et al.* (1987) and enriched for poly(A)+ using Oligotex suspension (Qiagen, Chatsworth, CA). After agarose gel electrophoresis, nucleic acids were transferred to Nylon membranes (Schleicher and Schuell, Keene, NH) as recommended by the manufacturer. DNA probes were radiolabeled with α-^{32}P dCTP (Amersham, Oakville, ON) by random priming using the T7 quick prime kit (Pharmacia, Baie d'Urfe, PQ).

Chromosome walk and restriction fragment length polymorphism (RFLP) mapping: A *pyr-4*-containing cosmid was isolated from the *N. crassa* Orbach-Sachs genomic cosmid library [obtained from the Fungal Genetics Stock Center (FGSC), Kansas City, KS] from 74-OR-23-1V (FGSC 2489; *het-C^{OR}*) strain using a *pyr-4* plasmid (pFB6; BUXTON and RADFORD 1983) as a probe. A chromosome walk was initiated in both directions using end fragment RNA probes generated by T3 or T7 polymerase (ORBACH 1994). Each cosmid from the walk mapped to the left arm of LGII, the known location of *het-C* and *pyr-4*, by RFLP mapping (METZENBERG *et al.* 1985).

Transformation assay for heterokaryon incompatibility: *N. crassa* spheroplasts were prepared according to the method of SCHWEIZER *et al.* (1981). The *het-C^{OR}* subclones were inserted into the pCB1004 vector conferring hygromycin resistance (CARROLL *et al.* 1994). For each construct, 20–30 *N. crassa* transformants were transferred to Vogel's slants containing hygromycin (250 units/ml) and incubated at 30° for 3 days. The appearance of the slow-growing, curly, aconidiating colonies was characteristic of the *het-C^{OR}/het-c^{PA}* incompatible reaction.

***Tn5* mutagenesis and subcloning of *het-C^{OR}*:** The *het-C^{OR}* cosmid, G22:H5, was submitted to *Tn5* mutagenesis as described by DE BRUIJN and LUPSKI (1984). The G22:H5:Tn5-mutated cosmids were transformed into *het-C^{OR}* and *het-c^{PA}* spheroplasts to test for *het-C^{OR}* activity. The positions of the *Tn5* insertions in the G22:H5 cosmid were determined by restriction fragment mapping and sequencing of the insertion point.

DNA sequence determination and reverse transcriptase (RT)-PCR: A series of overlapping subclones spanning the 3.9-kb *PstI-SacI het-C^{OR}*-containing fragment were obtained and sequenced on both strands using the ABI automated sequencing procedure (Mississauga, ON) at the NAPS unit, Biotechnology Laboratory, U.B.C. For RT-PCR, cDNA was synthesized using the First Strand cDNA synthesis kit (Pharmacia, Baie d'urfe, PQ) according to FERREIRA *et al.* (1996). For PCR, one-tenth of the cDNA synthesis reaction was amplified. Primers used were as follows: (462) 5′ACGATGACGGGTCTCAGG3′ (479) and (1200) 5′AAGGCCTCGCACAGGTCG3′ (1182) (see Figure 4). The *het-C^{OR}* amplification product was cloned into the pCRII vector using the TA cloning kit (Invitrogen, San Diego, CA) and sequenced as above.

RESULTS

Cloning of *het-C^{OR}*: The *het-C* locus is located on the left arm of LGII, ~1 map unit centromere distal to *pyr-4* (PERKINS *et al.* 1982) (Figure 2A). A *pyr-4*-containing cosmid (X7:F1) was isolated using the cloned *pyr-4* gene (BUXTON and RADFORD 1983), and a chromosome walk was extended from X7:F1 in both directions. Six overlapping cosmids covering a 150-kb region around *pyr-4* were isolated (Figure 2B).

Our initial strategy to locate the *het-C* locus within the cosmid walk was to use transformation to create synthetic partial diploids (transformation in *N. crassa* mainly occurs through integration at ectopic sites). Synthetic partial diploids heterozygous for *het-C* should display the *het-C^{OR}/het-c^{PA}* incompatibility phenotype as compared to transformants homozygous for *het-C*. However, it is possible that the introduction of a number of sequences into spheroplasts to form synthetic partial diploids could result in vegetative growth abnormalities. Therefore, a genetic approach was undertaken both to orient the chromosome walk and to pinpoint the location of *het-C* to a particular cosmid.

A cross was performed between two parental strains that showed RFLPs in the region of the chromosome

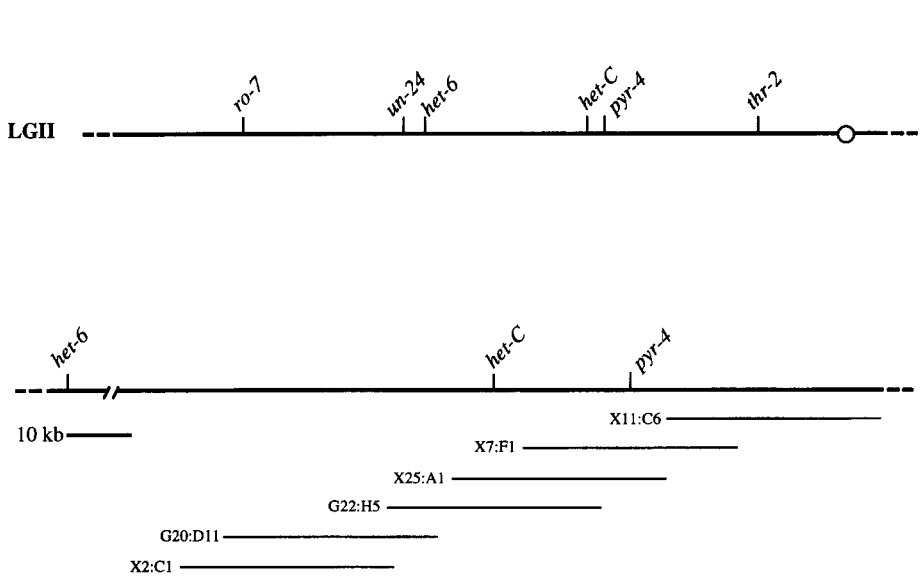

FIGURE 2.—Partial genetic map of linkage group II and cosmid walk from the *pyr-4* marker. (A) A partial genetic map of the left arm of linkage group II is depicted. (B) The extent of the cosmid walk from *pyr-4*.

walk, RLM 58-18 (*het-6^{PA} het-c^{PA} pyr-4; inl a*) and DJJ987-51 (*ro-7 un-24 het-6^{SP} het-C^{OR} thr-2 A*) (Table 1). Progeny that contained crossover points between *pyr-4*, a marker centromere proximal to *het-C*, and *un-24*, a centromere distal marker (Figure 2A), were selected by plating ascospores on threonine-containing medium at 37° (restrictive temperature for *un-24*). Sixty-five *un-24^{+}, pyr-4^{+}, thr-2^{-}* progeny were tested for their *het-C* genotype with *het-C* testers 6-19, 6-28, RLM 58-18 and 6-13 (Table 1). Sixty-two of the progeny were *het-C^{OR}*, indicating crossovers had occurred between *un-24* and *het-C* (Figure 3A). Three of the progeny were *het-c^{PA}*, indicating a crossover had occurred between *het-C* and *pyr-4* (25, 39, 64; Figure 3, A and B).

DNA from 55 progeny (52 *het-C^{OR}* and the three *het-c^{PA}*) was isolated and screened in a Southern blot using a probe made from the *pyr-4* cosmid, X7:F1. All three *het-c^{PA} pyr-4^{+}* progeny gave hybrid patterns when probed with X7:F1 that was distinct from the RFLPs exhibited by the parental strains (25, 39, 64; Figure 3A). When these same three progeny were probed with cosmids distal to X7:F1 (G22:H5 and X2:C1; Figure 2B), a pattern identical to the 58-18 (*het-c^{PA}*) parent was observed (Figure 3, A and B). These hybridization results not only oriented one arm of the walk toward the left telomere but indicate that the *het-C* locus is distal to the crossover points identified by X7:F1 in progeny 25, 39 and 64 (Figure 3B).

Recombination points were detected by the X7:F1 probe in all three of the progeny containing a crossover between *het-C* and *pyr-4*. These results suggested that the *het-C* locus may be closely linked physically as well as genetically to the *pyr-4* locus. To bracket the *het-C* locus within the cosmid walk, we needed to detect crossovers distal to the *het-C* locus, between *het-C* and *un-24*. When the 55 progeny were probed with G22:H5, a cosmid that is centromere distal to X7:F1 (Figure 2B), three of the 52 *het-C^{OR}* progeny (46, 50 and 51) exhibited hybrid RFLP patterns (Figure 3, A and C). These results indicate that a crossover occurred in 46, 50 and

TABLE 1

***N. crassa* strains**

Strain	Genotype	Origin
74-OR23-1VA	*het-C^{OR}A*	FGSC 2489
RLM 58-18	*het-6^{PA}het-c^{PA}pyr-4; inl a*	R. L. METZENBERG
DJJ987-51	*ro-7 un-24 het-6^{SP}het-C^{OR}thr-2 A*	D. J. JACOBSON
6-13	*ad3B arg-1; het-6^{PA}het-c^{PA}pyr-4 A*	C. YANG
6-19	*ad3B arg-1; het-6^{PA}het-C^{OR}; inl a*	C. YANG
6-28	*ad3B arg-1; het-6^{PA}het-C^{OR}; inl A*	C. YANG
c2(2)-9	*het-6^{PA}het-C^{OR}thr-2 A*	M. L. SMITH
c2(2)-1	*het-6^{PA}het-C^{OR}thr-2 a*	M. L. SMITH
c2(2)-25	*het-6^{PA}het-c^{PA}thr-2 A*	M. L. SMITH
c2(2)-5	*het-6^{PA}het-c^{PA}thr-2 a*	M. L. SMITH
c9-2	*het-6^{OR}het-c^{PA}thr-2 a*	M. L. SMITH

A

Isolate #	*het-C*	cosmid RFLP		
		X2:C1	G22:H5	X7:F1
25	PA	PA	PA	HY
39	PA	PA	PA	HY
64	PA	PA	PA	HY
46	OR	PA	HY	OR
50	OR	PA	HY	OR
51	OR	HY	HY	OR
26	OR	HY	OR	OR
36	OR	HY	OR	OR
42	OR	HY	OR	OR
49	OR	HY	OR	OR
60	OR	HY	OR	OR
68	OR	HY	OR	OR
75	OR	HY	OR	OR
76	OR	HY	OR	OR

C

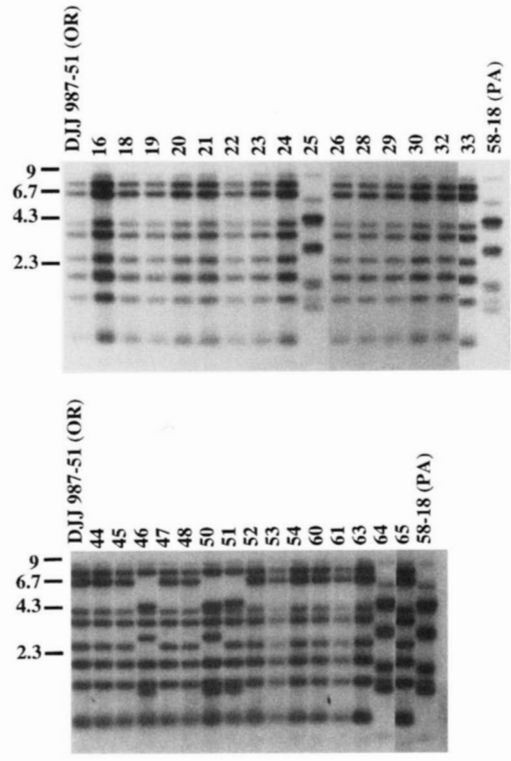

B

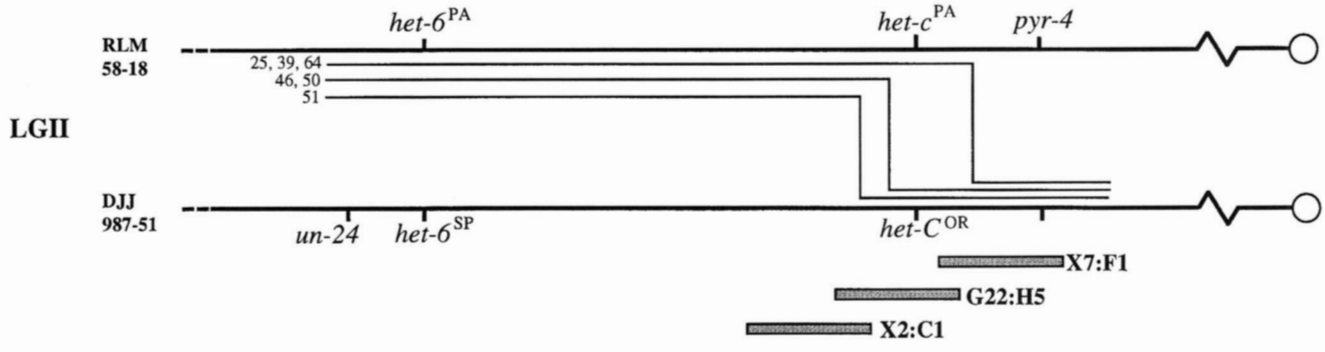

FIGURE 3.—Bracketing of *het-C* by recombination. (A) The RFLP patterns detected by three cosmids (X2:C1, G22:H5 and X7:F1; Figure 2B) for progeny with crossovers between *pyr-4* and *un-24*. Progeny in which crossovers were detected with at least one of the three cosmids are listed. OR, PA and HY stand for Oak Ridge, Panama and hybrid RFLP patterns, respectively. (B) A schematic interpretation of the hybridization results. The positions of the recombination points in progeny 25, 39, 64, 46, 50 and 51 relative to cosmids X2:C1, G22:H5 and X7:F1 are indicated. (C) The result of a Southern hybridization for 30 of the 55 crossover progeny and the parental strains (RLM 58-18 and DJJ987-51; Table 1) using the G22:H5 cosmid as a probe. Position of size standards is given in kb.

51 on the centromere distal side of the *het-C* locus, within the sequences detected by the G22:H5 probe (Figure 3B). The *het-C* locus was thus bracketed between the crossover points detected by X7:F1 and by G22:H5. When the 52 *het-C*^{OR} progeny were probed with X2:C1, a cosmid centromere distal to G22:H5, progeny 46 and 50 displayed a pattern identical to the *het-c*^{PA} parent (Figure 3A). Consistent with the fact that X2:C1 was found to be centromere distal to G22:H5, eight additional *het-C*^{OR} progeny that typed as Oak Ridge with the G22:H5 probe displayed a hybrid pattern when the X2:C1 cosmid was used as a probe (Figure 3A). The remainder of the 41 *het-C*^{OR} progeny presumably contained crossover points between *het-C*^{OR} and *un-24* that were centromere distal to the sequences surveyed by the chromosome walk.

The above results indicated that the *het-C* locus was on either X7:F1 or G22:H5 or both (in the region of overlap). To test this hypothesis, cosmids G22:H5, X25:A1 and X7:F1 (Figure 2B) were introduced into *het-C*^{OR} (c2(2)-1) and *het-c*^{PA} (c9-2) spheroplasts. The c2(2)-1 (*het-C*^{OR}) transformants containing X7:F1, X25:A1 and G22:H5 cosmids were similar in phenotype to transformants containing the pCB1004 (Hyg^{R}) vec-

tor. The c9-2 (*het-c*^{PA}) transformants carrying X7:F1 were also similar to vector controls. However, c9-2 transformants containing G22:H5 and X25:A1 yielded slow-growing, curly, nonconidiating colonies resembling *het-C* incompatible heterokaryons or partial diploids (Figure 1). These transformation results showed that the *het-C* locus resided in the region of overlap between G22:H5 and X25:A1, but not within the region of overlap with X7:F1 (Figure 2B).

To further locate *het-C*^{OR} on the G22:H5 cosmid, we performed *Tn5* insertional mutagenesis. It was reasoned that a *Tn5* insertion in the *het-C*^{OR} allele would abolish the capacity to confer the incompatible phenotype when introduced into *het-c*^{PA} spheroplasts. Seventeen G22:H5 *Tn5*-containing cosmids were introduced into *het-C*^{OR} and *het-c*^{PA} spheroplasts. One of the *Tn5* mutants (G22:H5:Tn11) gave normal transformants when introduced into both *het-C*^{OR} (c2(2)-1) and *het-c*^{PA} (c9-2) spheroplasts. The position of the *Tn5* insertion point in G22:H5 was determined by restriction mapping and was found to be located in the region of overlap between X25:A1 and G22:H5. Subclones spanning this insertion point were generated from the G22:H5 cosmid and tested for *het-C*^{OR} activity by transformation experiments. A fragment that conferred *het-C*^{OR} activity was thus subcloned as a 3.9-kb *Pst*I-*Sac*I fragment. Introduction of the 3.9-kb *Pst*I-*Sac*I subclone into *het-c*^{PA} spheroplasts gave Hyg^{R} transformants that exhibited a *het-C* incompatible phenotype that was indistinguishable from that of the G22:H5 cosmid and very similar to that exhibited by *het-C* incompatible heterokaryons or partial diploids (Figure 1).

Characterization of *het-C*^{OR}: The DNA sequence of the 3.9-kb *Pst*I-*Sac*I fragment was determined and found to contain a 966-amino acid (aa) open reading frame (ORF) interrupted by two putative introns of 65 and 64 bp, respectively (Figure 4). The sequence of the first 65 bp intron 5′ splice site is in poor agreement with the consensus sequences for *N. crassa* introns (GC AAGT as compared to GTAAGT consensus) (EDELMANN and STABEN 1994), and therefore the presence and position of the first intron was confirmed by sequencing a cDNA obtained by RT-PCR that spanned the intron position. The sequence of 5′ and 3′ splice site and lariat formation site of the proposed second intron are in good agreement with the consensus sequences. Sequences surrounding the ATG start codon are also in agreement with the consensus sequences for *N. crassa* translation start sites (EDELMANN and STABEN 1994). At 127 bp upstream of the ATG start codon, a sequence matching the consensus for transcription initiation sites in *N. crassa* was found (5′TCATCANC 3′; BRUCHEZ *et al.* 1993). No sequences matching the CAAT box or TATA box consensus were identified.

To confirm that the *Tn5* insertion in the G22:H5 cosmid that eliminated *het-C*^{OR} activity affected the 966-aa ORF, the location of the *Tn5* insertion point in the G22:H5 cosmid was determined. The *Tn5* insertion was at position 300, 164 bp upstream of the proposed ATG start codon and 37 bp upstream of the proposed transcriptional start site (Figure 4). It is likely the insertion of the *Tn5* transposon in the G22:H5 cosmid inactivates *het-C*^{OR} by preventing proper transcriptional initiation for the 966-aa ORF. The amino-terminal portion of the predicted 110-kD HET-C^{OR} contains an amino acid sequence that has good alignment with parameters identified from proteins with functional signal peptides (Figure 5A). The requirements for entering the secretory pathway include a positively charged amino-terminal region (n region), followed by an uninterrupted stretch of aliphatic amino acids (h region) and a more polar region (c region) with small residues (A and G) preferentially found at the −3 and −1 positions with respect to the signal peptidase cleavage site (NOTHWEHR and GORDON 1989; GIERASCH 1989). The n region of the signal peptide of HET-C^{OR} has a net positive charge, followed by 12 hydrophobic residues with a proline residue at position 23. Alanine residues are present at position 26 and 28, and a glycine residue is present at position 30, suggesting that processing of the signal peptide could occur either at position 29 or 31.

A region from amino acid position 426 to 458 in HET-C^{OR} contains a heptad repeat structure (with hydrophobic residues at positions **a** and **d** of the heptad) (Figure 5B). This motif is found in protein domains organized in a coiled-coil structure. The heptad repeats group hydrophobic residues on the same side of the ∝-helix. This structure is found as a dimerization motif (first termed "leucine-zipper") in several transcriptional regulators and in fibrous structural proteins such as intermediate filament proteins or myosin ("coiled-coil" structure per se) (PABO and SAUER 1992; FUCHS and WEBER 1994). Leucine-zippers are generally composed of four to five heptads, while the coiled-coil domains of fibrous proteins are much longer. The proposed coiled-coil domain of HET-C^{OR} is five heptads long and contains only hydrophobic residues in the **a** and **d** positions with some charged residues in the **e** and **g** positions (Figure 5B). Charged residues in the **e** and **g** positions are thought to stabilize interactions between neighboring helices (SIMONDS *et al.* 1993).

The carboxyl-terminal third of the predicted HET-C^{OR} is strikingly biased in amino acid composition. It is glycine-rich; 28% of the amino acids from position 610 to 966 are glycine. Other frequent amino acids in this region are tyrosine, serine and proline (together, 41% of the amino acid content). This region is hydrophilic and nearly devoid of aliphatic amino acids. A sequence from position 690 to 852 is particularly rich in proline (21% of the amino acid content). The carboxyl-terminal region of HET-C^{OR} is further characterized by repetitions of short amino acid motifs; eight repeats (partial or perfect) of the SQPSYG motif and six repeats of the GGYGG motif are found from amino acid posi-

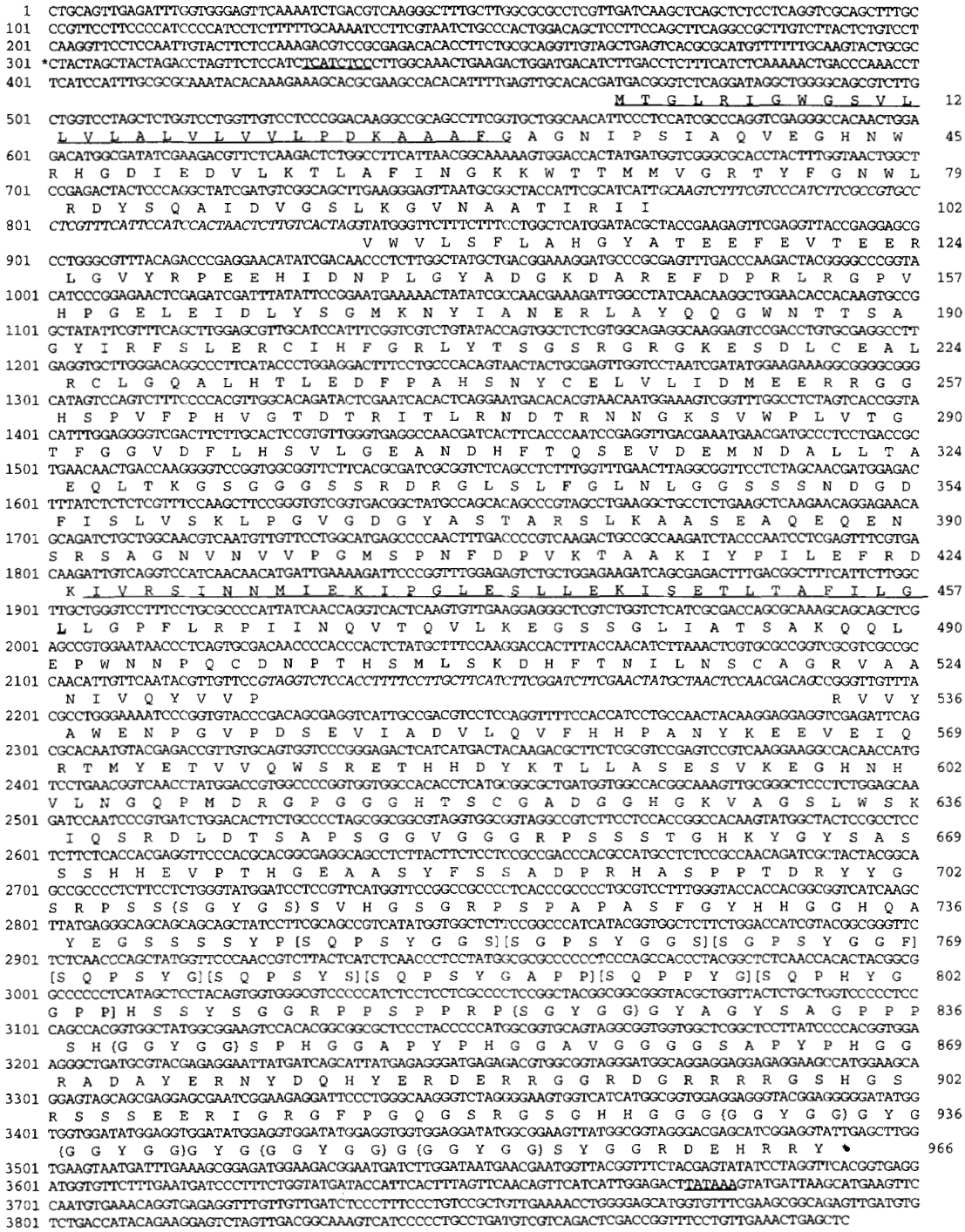

FIGURE 4.—Nucleotide sequence of the 3.9-kb *Pst*I-*Sac*I *het-C*^{OR} fragment and translation of the proposed *het-C*^{OR} ORF. Intron sequences are italicized. Sequences matching the consensus for the transcriptional start site and poly(A) tail addition site are underlined. The position of the insertion point of the *Tn5* transposon is shown by *. The proposed signal peptide and coiled-coil region are underlined. The two types of repeats in the glycine-rich domain are bracketed ({ } for the GGYGG motif and [ ] for the SQPSYG motif). The accession number for this sequence is L77234.

tions 708 to 951 (Figure 4). The sequence of the predicted HET-C^{OR} was compared to protein sequences using the BLAST algorithm (ALTSCHUL *et al.* 1990). The glycine-rich domain was found to be similar to glycine-rich domains found in various extracellular or cell envelope proteins, such as plant cell wall glycine-rich proteins (SHOWALTER 1993; ROHDE *et al.* 1990), a cell envelope protein of keratinocytes (MEHREL *et al.* 1990) and eggshell proteins from invertebrates (BOBEK *et al.* 1986). Glycine-rich domains are also found in intracellular RNA-binding proteins (SHOWALTER 1993) and end domains of keratins K1 and K10, specific for terminally differentiated epidermis (FUCHS and WEBER 1994). All of these polypeptides share the same bias in amino acid

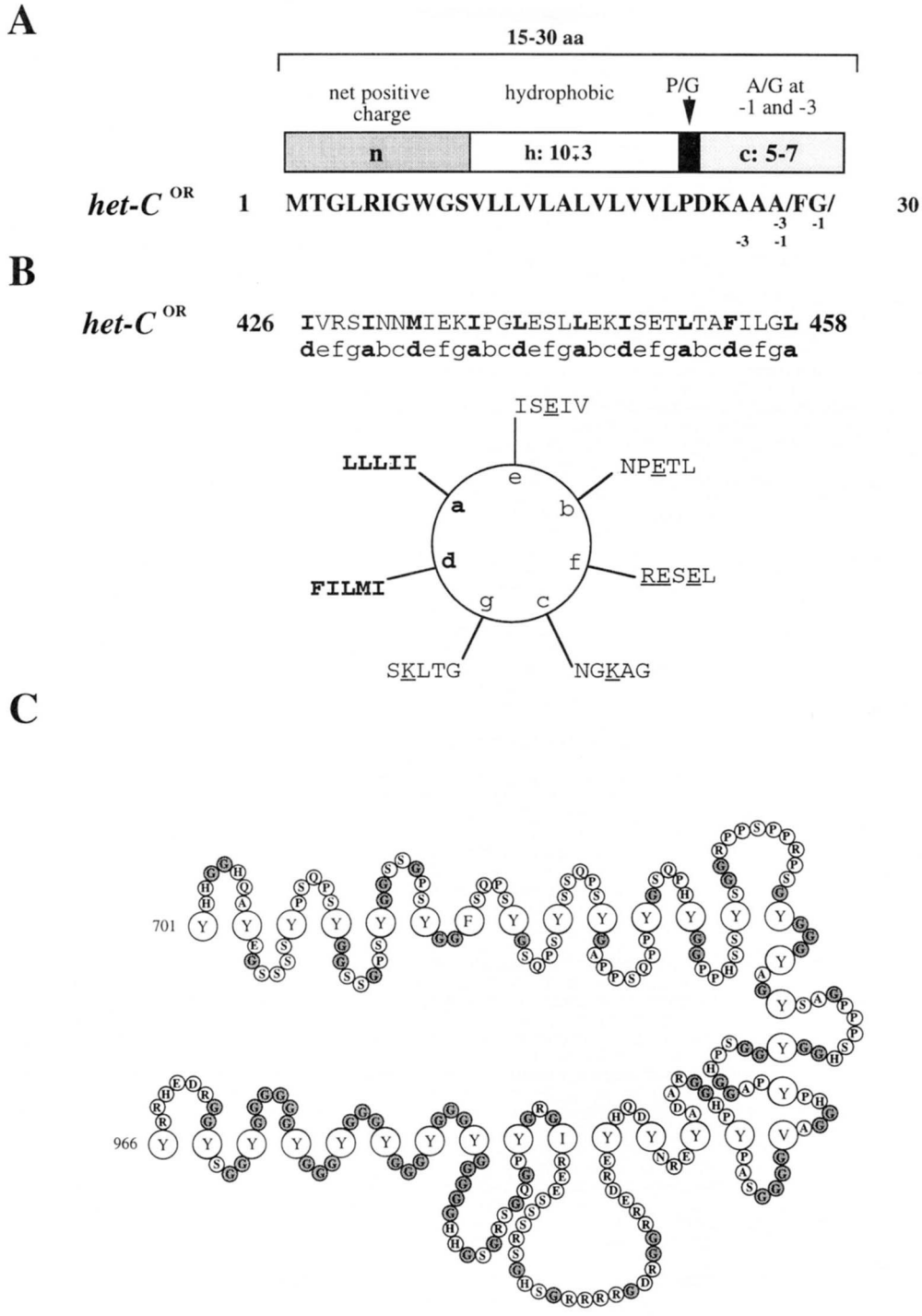

FIGURE 5.—Sequence features of the *het-C*^{OR}-encoded polypeptide. (A) Comparison of the N-terminal sequence of the proposed *het-C*^{OR}-encoded polypeptide with the consensus structure defined for signal peptides. The consensus sizes for the h and c regions are given. The positions of the proposed cleavage sites are shown by / and the −3 and −1 positions with respect to those cleavage sites are indicated. (B) The sequence of the coiled-coil heptad repeat structure of HET-C^{OR} (top) together with a helical wheel representation of the same region (bottom). The hydrophobic residues of the heptad repeat are in bold and charged residues are underlined. (C) The proposed structure of the glycine-rich domain of HET-C^{OR} from position 701 to 966 according to the model of STEINERT *et al.* (1991). The stacked aromatic residues (and occasional long chain aliphatic residues) are represented as larger circles and glycine residues are shaded. The bending of the aromatic residue stack is depicted only to simplify schematic representation.

composition and contain oligopeptide repetitions similar or identical to the repeats found in the *het-C*^{OR}-encoded polypeptide. In addition to the abundance of glycine residues, these domains are characterized by relatively regularly spaced aromatic residues (mainly tyrosine and phenylalanine). It has been proposed that

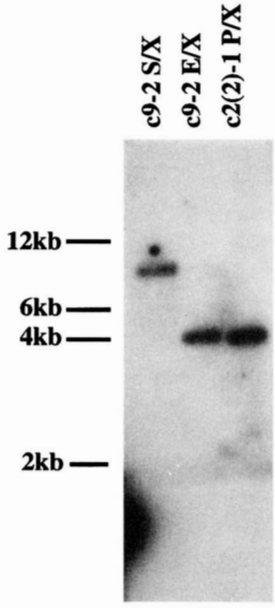

FIGURE 6.—Hybridization of the cloned *het-C*^{OR} to genomic DNA from *het-C*^{OR} and *het-c*^{PA} DNA. Genomic DNA from the c9-2 (*het-c*^{PA}) and c(2)2-1 (*het-C*^{OR}) strains was digested and probed with the *het-C*^{OR} 3.9-kb *Sac*I-*Pst*I fragment (E, *Eco*RI; P, *Pst*I; S, *Sac*I; X, *Xba*I). Position of size standards is given on the left.

these sequences adopt a structure in which the side chains of the aromatic residues (and occasional long chain aliphatic residues) are stacked, forcing the glycine-rich intervening stretches to loop out (STEINERT *et al.* 1990). This structure (glycine-loop domain) is predicted to be highly flexible and dynamic. The glycine-loop domain has been proposed to allow tension-adaptable protein-protein interactions that provide extensibility and elasticity to the animal epidermis (STEINERT *et al.* 1990). Figure 5C shows a representation of the glycine-rich domain of the *het-C*^{OR} product according to the glycine-loop model. In good agreement with this model, the glycine-rich domain of HET-C^{OR} is predicted to have a very low content of α-helical or β-strand secondary structures.

Copy number and hybridization of *het-C*^{OR} clone to *het-C*^{OR} and *het-c*^{PA} genomic DNA: The 3.9-kb *Pst*I-*Sac*I fragment was used as a probe in DNA hybridization experiments to genomic DNA isolated from both *het-C*^{OR} and *het-c*^{PA} strains. Under conditions of high stringency, only a single copy of the *het-C* locus is present in the genome of *het-C*^{OR} strains (Figure 6 and data not shown). Hybridization to the *het-C*^{OR} allele was also detected as a single copy in *het-c*^{PA} genomic DNA, suggesting that a high degree of sequence similarity is present between the alternate alleles (Figure 6).

Isolation of *het-C*^{OR} RIP mutants: Mutants of *het-C*^{OR} were obtained by RIP (SELKER 1990), a mechanism that causes repeated sequences to undergo multiple G-C to A-T transition mutations before karyogamy during a cross. The *c2(2)-1* (*het-C*^{OR}) strain was transformed with 2.2-kb *Eco*RV-*Kpn*I *het-C*^{OR} fragment that encompasses an internal portion (611-2780, Figure 4) of the 966-aa *het-C*^{OR} ORF. An internal fragment of the *het-C*^{OR} ORF was used because it is known that RIP can spread outside of the duplicated region (SELKER 1991). A homokaryotic transformant (Y2) was recovered after three rounds of single conidial isolations and crossed with the *c2(2)-9* strain. It has been shown that RIP frequencies are higher in ascospores recovered late from a cross (SINGER *et al.* 1995a). Therefore, late ascospores shot 12–15 days after fertilization were recovered and 41 such progeny were analyzed. The hygromycin-resistance marker and mating type segregated 1:1 in all 41 progeny. The *het-C* genotype was analyzed in the 41 progeny by forcing heterokaryons with *het-c*^{PA} and *het-C*^{OR} testers (6-13, 58-18, 6-28, 6-19; Table 1). Seven progeny were found to be compatible with both *het-c*^{PA} and *het-C*^{OR} testers (Figure 7A). The dual-compatible strains did not display any obvious mutant phenotype during vegetative growth or sexual reproduction and were similar in all respects to the wild-type parental strains.

To test the segregation of the *het-C* compatible phenotype, one of the dual-compatible strains (Y2.7) (*thr-2*) was crossed with 6-13 (*ad-3B arg-1; het-6*^{PA} *het-c*^{PA} *pyr-4 A;* Table 1). All *pyr-4*$^{+}$ progeny were compatible with both *het-c*^{PA} and *het-C*^{OR} testers, a phenotype identical to that of the Y2.7 parent. The Y2.7 strain was also crossed to *c(2)2-9 het-C*^{OR} strain; one-half of the progeny exhibited the dual-compatible phenotype and one-half typed as *het-C*^{OR}. Results from both of these crosses with Y2.7 show that the mutation responsible for dual-compatibility is closely linked to the *het-C* locus.

In addition to transition mutations, RIP is also associated with methylation of altered sequences (SINGER *et al.* 1995b). To confirm that the dual-compatible mutants suffered RIP mutations within the *het-C*^{OR} allele, they were analyzed at the molecular level to detect RIP-induced RFLP alterations and associated methylation. Genomic DNA from three dual-compatible progeny was digested by *Mbo*I and *Sau*3A and analyzed in a Southern blot using a 2.8-kb *Pst*I-*Kpn*I *het-C*^{OR} fragment as a probe. *Mbo*I and *Sau*3A are isoschizomers, but *Sau*3A is sensitive to methylation whereas *Mbo*I is not. In all of the dual-compatible mutants, RFLP and/or methylation were detected in the 2.8-kb *Pst*I-*Kpn*I fragment (Figure 7B and data not shown), indicating that the mutant phenotype resulted from RIP of the *het-C*^{OR} allele. The RIP frequency of the *het-C*^{OR} allele was 34%, a frequency comparable to those previously reported for late ascospores (SINGER *et al.* 1995a).

Functional analysis of *het-C*^{OR}: The RIP analyses and transformation results indicated that the 3.9-kb *Pst*I-*Sac*I fragment encoded the *het-C*^{OR} allele. We therefore chose to examine further the domains of the 966-aa ORF required to confer *het-C*^{OR} activity. Several deletion and frame shift *het-C*^{OR} constructs were obtained and tested for *het-C*^{OR} activity by introduction into *het-C*^{OR} and *het-*

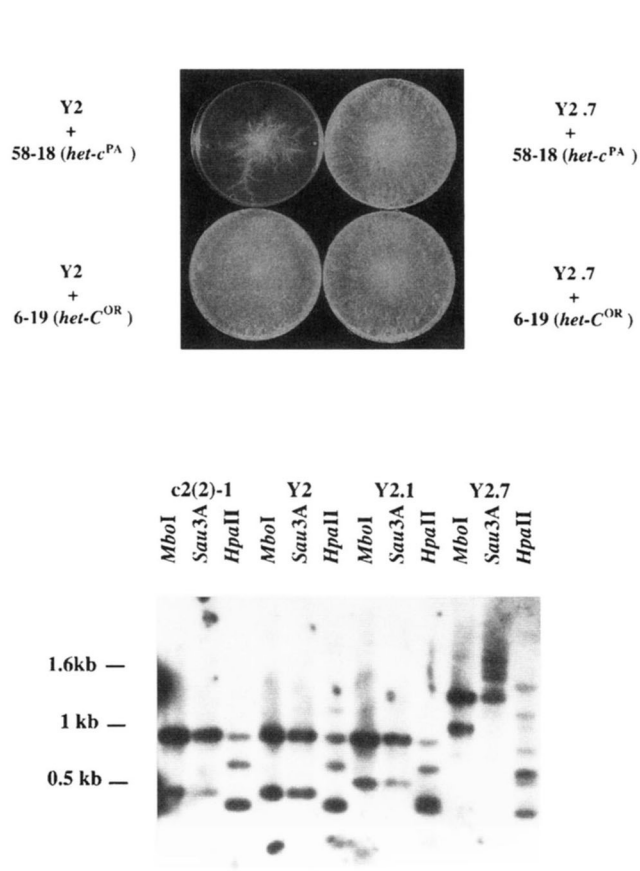

FIGURE 7.—Growth characteristics of heterokaryons with *het-C*^{OR} RIP mutants. (A) The phenotype of heterokaryons of the Y2 strain (*het-C*^{OR}/*het-C*^{OR} transformant) and RIP progeny, Y2.7, with *het-C*^{OR} and *het-c*^{PA} testers. Strains were grown for 3 days on minimal solid Vogel's medium. Designations of the tester strains are given. (B) The result of a Southern hybridization using the 2.8-kb *Pst*I-*Sma*I *het-C*^{OR} fragment as a probe. Y2 is the original transformant; Y2.1 and Y2.7 are two different dual-compatible progeny from the RIP cross. DNA was digested with *Mbo*I, *Sau*3A; *Hpa*II, an additional a methylation-sensitive four base cutter, was also used. Position of size standards is given on the left.

c^{PA} spheroplasts (Figure 8). A +1 frame-shift mutation at codon position 120 abolished *het-C*^{OR} activity, confirming that the 966-aa ORF encodes HET-C^{OR}. To examine the requirement for the glycine-rich domain, two deletion constructs that removed various lengths of the carboxyl-terminal portion of HET-C^{OR} were obtained and tested for *het-C*^{OR} activity. When the last 237 codons of the *het-C*^{OR} ORF were deleted, *het-C*^{OR} activity was retained. The deleted region corresponded to ~2/3 of the glycine-rich domain including the repeated regions. Deletion of the last 385 codons (581–966) abolished activity (Figure 8). This deletion removed the entire glycine-rich domain and 30 amino acids N-terminal to that domain. This suggested that the region between amino acid position 581 and 729 is essential in triggering the *het-C* incompatibility response.

The functional significance of the proposed coiled-coil domain of HET-C^{OR} was tested by making an in-frame deletion construct (*het-C*^{OR}lz) that removed the 70-aa region (420–491) containing the entire 33-aa long proposed coiled-coil (Figure 8). The *het-C*^{OR}lz construct yielded only ~10% incompatible colonies upon introduction into *het-c*^{PA} spheroplasts and the incompatible phenotype of the *het-C*^{OR}lz/*het-c*^{PA} transformants was less severe than that observed in the *het-C*^{OR}/*het-c*^{PA} transformants.

DISCUSSION

We have cloned and characterized the *het-C*^{OR} allele of the *het-C* incompatibility locus of *N. crassa* using positional cloning and a functional assay. RIP mutants of the *het-C*^{OR} allele were obtained. These displayed dual-compatibility with both *het-C*^{OR} and *het-c*^{PA} strains but were otherwise indistinguishable from wild type.

The 966-aa *het-C*^{OR} predicted polypeptide possesses a signal peptide sequence. The *het-C*^{OR} product is thus expected to enter the secretory pathway. Hydrophobic regions predicted to form transmembrane α-helixes were not detected, and it is therefore unlikely that HET-C^{OR} is an integral membrane protein. The hydrophilic glycine-rich C-terminal domain of HET-C^{OR} is similar to glycine-rich domains found in a number of extracellular or cell envelope proteins (SHOWALTER 1993; BOBEK *et al.* 1986; MEHREL *et al.* 1990). These features suggest that HET-C^{OR} is an extracellular glycine-rich protein associated with the fungal cell wall.

Spatial and temporal regulation of cell wall assembly is essential in fungal growth and development. Colony morphology in filamentous fungi is believed to be primarily controlled by cell wall structure, and numerous morphological mutants in *N. crassa* have been found to be affected in cell wall determinants (MISHRA 1977). It is possible that the altered growth and morphology of the *het-C*^{OR}/*het-c*^{PA} incompatible heterokaryons or partial diploids could result from an effect on cell wall structure or organization. Imbalances during the developmental process of hyphal fusion or modifications in the components of cell wall assembly would drastically affect the growth and morphology of an incompatible heterokaryon.

The simplest model describing how *het* genes trigger incompatibility predicts protein-protein interaction between alternate *het* gene products. The putative *het-C*^{OR} product contains a coiled-coil structure, and a combinatorial interaction of proteins has been shown to be mediated by such structures in several instances (O'SHEA *et al.* 1992; HO *et al.* 1994; KAMLPER *et al.* 1995). Our working model predicts direct protein-protein interaction between alternate *het-C* gene products via this domain. The formation of a HET-C^{OR}/HET-c^{PA} heterodimer would then lead to a growth inhibition and morphological alterations in the resulting heterokar-

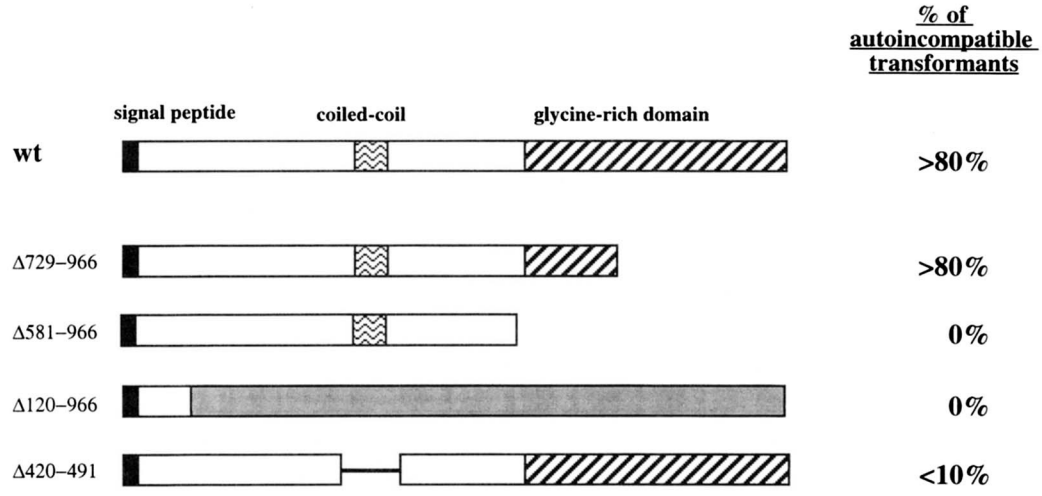

FIGURE 8.—Activity of *het-C*^{OR} deletion and frame shift constructs. A schematic of the structure of different *het-C*^{OR} deletion (Δ) and frame shift constructs (fs) is depicted. Extent of the deletions and the position of the frame shift mutation are given. The results of the transformation assay for *het-C*^{OR} activity are given as percentages of auto-incompatible transformants. At least 30 transformants were individually tested for each construct.

yon. The introduction of a construct bearing a deletion of the HET-C^{OR} coiled-coil domain into *het-c*^{PA} spheroplasts gave compatible transformants, although a small percentage displayed a slight *het-C* auto-incompatible phenotype. These results suggest that other parts of HET-C^{OR} allow HET-C^{OR}/HET-c^{PA} interaction in addition to the coiled-coil domain. This phenotype could also be caused by a variation in the expression level of the transgene in different transformants due to differences in copy number and/or integration site. The deletion of this region may also affect protein folding or stability of the *het-C*^{OR}1z product.

Early studies on *het-C* showed that cells can be killed by microinjection of cytoplasm from an incompatible donor cell (WILSON *et al.* 1961). These results are in apparent contrast with the proposed extracellular location of the *het-C*^{OR} product. However, in those studies some *het-C* incompatible microinjections failed to kill recipient cells. The existence of a second *het* locus very closely linked to *het-C* has been postulated (HOWLETT *et al.* 1993; S. SAUPE, unpublished results) and could account for these apparent contradictions. Moreover, modifier genes affecting heterokaryon compatibility have been recently identified in the strains used for the microinjection studies (JACOBSON *et al.* 1995).

Initial DNA sequence results with *het-C* indicate that the *het-C*^{OR} and *het-c*^{PA} alleles are very similar. Identity at the DNA level between the two alleles is >95% (S. SAUPE, unpublished results). Thus, *het-C*^{OR} and *het-c*^{PA} are true alleles rather than idiomorphs as in the case of mating type (GLASS *et al.* 1988). *het-C* resembles the allelic incompatibility locus, *het-s,* of the filamentous fungus, *Podospora anserina* in two respects. Both encode nonessential polypeptides and alternate alleles encode very similar, but not identical polypeptides (TURCQ *et al.* 1991; S. SAUPE, unpublished results).

It has been proposed that *het* genes were not primarily selected to limit heterokaryosis but encode proteins with cellular functions (BEGUERET *et al.* 1995). As a consequence of sequence divergence, altered protein complexes would be formed in heterokaryons and trigger incompatibility. This hypothesis is supported by the fact that mating type in *N. crassa* and a *P. anserina het* locus involved in nonallelic interactions, *het-c,* have cellular functions in addition to those of vegetative incompatibility (GLASS *et al.* 1990; STABEN and YANOFSKY 1990; SAUPE *et al.* 1994). The structure of the *het-C*^{OR} predicted polypeptide suggests that it may have a functional, although not essential, role in the fungal cell wall in addition to eliciting vegetative incompatibility.

Comparison of all *het* genes characterized so far does not reveal any obvious functional or structural similarities, suggesting that they do not have a common evolutionary origin. The *N. crassa mt A-1* and *mt a-1* genes responsible for mating type-associated incompatibility resemble transcriptional regulators (GLASS *et al.* 1990; STABEN and YANOFSKY 1990). In *P. anserina,* the *het-s*-encoded products have no detectable similarity to known proteins (TURCQ *et al.* 1991). The *het-e*-encoded polypeptide of *P. anserina* is similar to a glycolipid transfer protein and is required for proper ascospore formation (SAUPE *et al.* 1994). The *het-e* locus of *P. anserina* encodes a putative GTP-binding protein with β-transducin-like repeats (SAUPE *et al.* 1995). It appears that *het* genes may be involved in a variety of cellular processes and may elicit vegetative incompatibility by a number of different mechanisms. Although a number of *het* genes have been isolated, the molecular means of recognition remains unknown and the biochemical basis of the incompatibility response remains to be elucidated.

We thank DAVID JACOBSON for providing *N. crassa* strains and CAM WYNDHAM for providing *Tn5* oligonucleotides. We appreciate the

technical support of BEN LEE for transformation studies. We appreciate comments from DAVID PERKINS and DAVID JACOBSON on the manuscript. G.A.K. was a recipient of a Natural Sciences and Engineering Research Council (NSERC) International Postdoctoral Fellowship, and M.L.S. was the recipient of a Killam Postdoctoral Fellowship and an NSERC Postdoctoral Fellowship. This research was supported by a grant from the NSERC to N.L.G.

LITERATURE CITED

ALTSCHUL, S. F., W. GISH, W. MILLER, E. W. MYERS and D. J. LIPMAN, 1990 Basic logical alignment search tool. J. Mol. Biol. **215:** 403–410.

BEADLE, G. W., and V. L. COONRADT, 1944 Heterocaryosis in *Neurospora crassa*. Genetics **29:** 291–308.

BEGUERET J., B. TURCQ and C. CLAVE, 1995 Vegetative incompatibility in filamentous fungi: *het* genes begin to talk. Trend Genet. **10:** 441–446.

BOBEK, L., D. M. REKOSH, H. VAN KEULEN and P. T. LO VERDE, 1986 Characterization of a female-specific cDNA derived from a developmentally regulated mRNA in the human blood fluke *Schistosoma mansoni*. Proc. Natl. Acad. Sci. USA **83:** 5544–5548.

BRUCHEZ, J. J. P., J. EBERLE and V. E. A. RUSSO, 1993 Regulatory sequences in the transcription of *Neurospora crassa* genes: CAAT-box, TATAbox, introns, poly(A) tail formation sequences. Fungal Genet. Newslett. **40:** 89–96.

BUXTON, F., and A. RADFORD, 1983 Cloning of the structural gene for orotidine 5′-phosphate carboxylase of *Neurospora crassa* by expression in *Escherichia coli*. Mol. Gen. Genet. **190:** 403–405.

CARROLL, A. M., J. A. SWEIGARD and B. VALENT, 1994 Improved vectors for selecting resistance to hygromycin. Fungal Genet. Newslett. **41:** 22.

DAVIS, R. H., and F. J. DE SERRES, 1970 Genetic and microbial research techniques for *Neurospora crassa*. Methods Enzymol. **17A:** 79–143.

DE BRUIJN F. J., and J. R. LUPSKI, 1984 The use of transposon *Tn5* mutagenesis in the rapid generation of correlated physical and genetic maps of DNA segments cloned into multicopy plasmids-a review. Gene **27:** 131–149.

EDELMAN, S., and C. STABEN, 1994 A statistical analysis of sequence features within genes from *Neurospora crassa*. Exp. Mycol. **18:** 70–81.

FERREIRA, A. V. B., S. SAUPE and N. L. GLASS, 1996 Transcriptional analyses of the *A* idiomorph of *Neurospora crassa* identifies two genes in addition to *mt A-1*. Mol. Gen. Genet. **250:** 767–774.

FUCHS, E., and K. WEBER, 1994 Intermediate filaments: structure dynamics, function and disease. Annu. Rev. Biochem. **63:** 345–382.

GARNJOBST, L., 1953 Genetic control of heterokaryosis in *Neurospora crassa*. Am. J. Bot. **40:** 607–614.

GARNJOBST, L., and J. F. WILSON, 1956 Heterokaryosis and protoplasmic incompatibility in *Neurospora crassa*. Proc. Natl. Acad. Sci. USA **42:** 613–618.

GIERASCH, L. M., 1989 Signal sequences. Biochemistry **28:** 923–930.

GLASS, N. L., and G. A. KULDAU, 1992 Mating type and vegetative incompatibility in filamentous ascomycetes. Annu. Rev. Phytopathol. **30:** 201–224.

GLASS, N. L., S. J. VOLLMER, C. STABEN, J. GROTELUESCHEN, R. L. METZENBERG *et al.*, 1988 DNAs of the two mating-type alleles of *Neurospora crassa* are highly dissimilar. Science **241:** 570–573.

GLASS, N. L., J. GROTELUESCHEN and R. L. METZENBERG, 1990 *Neurospora crassa A* mating-type region. Proc. Natl. Acad. Sci. USA **87:** 4912–4916.

HO, C., J. G. ADAMSON, R. S. HODGES and M. SMITH, 1994 Heterodimerization of the yeast MAT**a1** and MATα2 proteins is mediated by two leucine zipper-like coiled-coil motifs. EMBO J. **13:** 1403–1413.

HOWLETT, B. J., J. F. LESLIE and D. D. PERKINS, 1993 Putative multiple alleles at the vegetative (heterokaryon) incompatibility loci *het-c* and *het-8* in *Neurospora crassa*. Fungal Genet. Newslett. **40:** 40–42.

JACOBSON, D. J., J. OHRNBERGER and R. A. AKINS, 1995 The Wilson-Garnjobst heterokaryon incompatibility tester strains of *Neurospora crassa* contain modifiers which influence growth rate of heterokaryons and distort segregation ratios. Fungal Genet. Newslett. **42:** 34–40.

KAMPLER, J., M. REICHMANN, T. ROMEIS, M. BOLKER and R. KAHMANN 1995 Multiallelic recognition: nonself-dependent dimerization of the *bE* and *bW* homeodomain proteins in *Ustilago maydis*. Cell **81:** 73–83.

LESLIE, J. F., 1993 Fungal vegetative compatibility. Annu. Rev. Phytopath. **31:** 127–150.

LOGEMANN, J., J. SCHELL and L. WILLMITZER, 1987 Improved method for the isolation of RNA from plant tissues. Anal. Biochem **163:** 16–20.

MEHREL, T., D. HOHL, J. A. ROTHNAGEL, M. A. LONGLEY, D. BUNDMAN *et al.*, 1990 Identification of a major keratinocyte cell envelope protein, loricrin. Cell **61:** 1103–1112.

METZENBERG, R. L., J. N. STEVENS, E. U. SELKER and E. MORZYCKA-WROBLEWSKA, 1985 Identification and chromosomal distribution of 5S RNA genes in *Neurospora crassa*. Proc. Natl. Acad. Sci. USA **82:** 2067–2071.

MISHRA, N. C., 1977 Genetics and biochemistry of morphogenesis in Neurospora. Adv. Genet. **19:** 314–405.

MYLYK, O. M., 1975 Heterocaryon incompatibility genes in *Neurospora crassa* detected using duplication-producing chromosome rearrangements. Genetics **80:** 107–124.

MYLYK, O. M., 1976 Heteromorphism for heterokaryon incompatibility genes in natural populations of *Neurospora crassa*. Genetics **83:** 275–284.

NOTHWEHR, S. F., and J. I. GORDON, 1989 Eukaryotic signal peptide structure/function relationships. J. Biol. Chem. **264:** 3979–3987.

OAKLEY, C. E., C. F. WEIL, P. L. KRETZ and B. R. OAKLEY, 1987 Cloning of the *riboB* locus of *Aspergillus nidulans*. Gene **53:** 293–298.

ORBACH, M. J., 1994 A cosmid with a HyR marker for fungal library construction and screening. Gene **150:** 159–162.

O'SHEA Y., E. K. R. RUTKOWSKI and P. S. KIM, 1992 Mechanism of specificity in the *Fos-Jun* oncoprotein heterodimer. Cell **68:** 699–708.

PABO, C. O., and R. T. SAUER, 1992 Transcription factors: structural families and principles of DNA recognition. Annu. Rev. Biochem. **61:** 1053–1095.

PERKINS, D. D., 1975 The use of duplication-generating rearrangements for studying heterokaryon incompatibility genes in Neurospora. Genetics **80:** 87–105.

PERKINS, D. D., 1988 Main features of vegetative incompatibility in Neurospora. Fungal Genet. Newslett. **35:** 44–46.

PERKINS, D. D., A. RADFORD, D. NEWMEYER and M. BJORKMAN, 1982 Chromosomal loci of *Neurospora crassa*. Microbiol. Rev. **46:** 426–570.

ROHDE, W., K. ROSCH, K. KROGER and F. SALAMINI, 1990 Nucleotide sequence of a *Hordeum vulgare* gene encoding a glycine-rich protein with homology to vertebrate cytokeratins. Plant Mol. Biol. **14:** 1057–1059.

SANSOME, E. R., 1946 Heterokaryosis, mating-type factors, and sexual reproduction in Neurospora. Bull. Torrey Bot. Club **73:** 397–409.

SAUPE, S., C. DESCAMPS, B. TURCQ and J. BEGUERET, 1994 Inactivation of the *Podospora anserina* vegetative incompatibility locus *het-c*, whose product resembles a glycolipid transfer protein, drastically impairs ascospore production. Proc. Natl. Acad. Sci. USA **91:** 5927–5931.

SAUPE, S., B. TURCQ and J. BEGUERET, 1995 A gene responsible for vegetative incompatibility in the fungus *Podospora anserina* encodes a protein with a GTP-binding motif and Gβ homologous domain. Gene **162:** 135–139.

SCHWEIZER M., M. E. CASE, C. C. DYKSTRA, N. H. GILES and S. R. KUSHNER, 1981 Identification and characterization of recombinant plasmids carrying the complete *qa* gene cluster from *Neurospora crassa* including the *qa-1+* regulatory gene. Proc. Natl. Acad. Sci. USA **78:** 5086–5090.

SELKER, E. U., 1990 Premeiotic instability of repeated sequences in *Neurospora crassa*. Annu. Review Genet. **24:** 579–613.

SELKER, E. U., 1991 Repeat-induced point mutation and DNA methylation, pp. 258–265 in *More Gene Manipulations in Fungi*, edited by J. W. BENNETT and L. L. LASURE. Academic Press, San Diego.

SHOWALTER, A. M., 1993 Structure and function of plant cell wall proteins. Plant Cell **5:** 9–23.

SIMONDS, W. F., H. K. MANJI and A. GARRITSEN, 1993 G proteins

and BARK: a new twist for the coiled coil. Trends Biol. Sci. **18:** 315–317.

SINGER, M. J., E. A. KUZMINOVA, A THARP, B. S. MARGOLIN and E. U. SELKER, 1995a Different frequencies of RIP among early *vs.* late ascospores of *Neurospora crassa.* Fungal Gen. Newslett. **42:** 74–75.

SINGER, M. J., B. A. MARCOTTE and E. U. SELKER, 1995b DNA methylation associated with repeat-induced point mutation in *Neurospora crassa.* Mol. Cell. Biol. **15:** 5586–5597.

STABEN, C., and C. YANOFSKY, 1990 *Neurospora crassa a* mating-type region. Proc. Natl. Acad. Sci. USA **87:** 4917–4921.

STEINERT, P. M., J. M. MACK, B. P. KORGE, S. GAN, S. R. HAYNES *et al.*, 1990 Glycine loops in proteins: their occurrence in certain intermediate filament chains, loricrins and single-stranded RNA binding proteins. Int. J. Biol. Macromol. **13:** 130–139.

TURCQ, B., C. DELEU, M. DENAYROLLES and J. BEGUERET, 1991 Two allelic genes responsible for vegetative incompatibility in the fungus *Podospora anserina* are not essential for cell viability. Mol. Gen. Genet. **228:** 265–269.

VOGEL, H. J., 1964 Distribution of lysine pathways among fungi: evolutionary implications. Am. Nat. **98:** 435–446.

WESTERGAARD, M., and H. K. MITCHELL, 1947 *Neurospora* V. A synthetic medium favoring sexual reproduction. Am. J. Bot. **34:** 573–577.

WILSON, J. F., L. GARNJOBST and E. L. TATUM, 1961 Heterocaryon incompatibility in *Neurospora crassa:* micro-injection studies. Am. J. Bot. **48:** 299–305.

Communicating editor: R. H. DAVIS